Mutational analysis of the N-linked glycosylation sites of the human insulin receptor

Thomas C. ELLEMAN, Maurice J. FRENKEL, Peter A. HOYNE, Neil M. McKERN, Leah COSGROVE, Dean R. HEWISH, Kim M. JACHNO, John D. BENTLEY, Sonia E. SANKOVICH and Colin W. WARD[1]

Commonwealth Scientific and Industrial Research Organisation, Division of Health Sciences and Nutrition, 343 Royal Parade, Parkville, Victoria 3052, Australia

Site-directed mutagenesis has been used to remove 15 of the 18 potential N-linked glycosylation sites, in 16 combinations, from the human exon 11-minus receptor isoform. The three glycosylation sites not mutated were asparagine residues 25, 397 and 894, which are known to be important in receptor biosynthesis or function. The effects of these mutations on proreceptor processing into α and β subunits, cell-surface expression, insulin binding and receptor autophosphorylation were assessed in Chinese hamster ovary cells. The double mutants 16+78, 16+111, 16+215, 16+255, 337+418, the triple mutants 295+337+418, 295+418+514, 337+418+514 and 730+743+881 and the quadruple mutants 606+730+743+881 and 671+730+743+881 seemed normal by all criteria examined. The triple mutant 16+215+255 showed only low levels of correctly processed receptor on the cell surface, this processed receptor being autophosphorylated in response to insulin. The quadruple mutant 624+730+743+881 showed normal processing and ligand binding but exhibited a constitutively active tyrosine kinase as judged by autophosphorylation. Three higher-order mutants were constructed, two of which, 16+337+418+730+743+881 (Δ6) and 16+295+337+418+730+743+881 (Δ7a), seemed normal. The third construct, 16+337+418+514+730+743+881 (Δ7b), was expressed at high levels on the cell surface, essentially as uncleaved proreceptor with only the small proportion of Δ7b that was correctly processed showing insulin-stimulated autophosphorylation. The mutations of Δ6 and Δ7a were incorporated into soluble ectodomains, which had affinities for insulin that were 4-fold that of wild-type ectodomain. The Δ6 ectodomain expressed in Lec8 cells was produced in quantity in a bioreactor for subsequent structural analysis.

Key words: autophosphorylation, biosynthesis, insulin binding, mutagenesis, protein folding.

INTRODUCTION

Glycosylation is a major source of molecular heterogeneity of glycoproteins in both composition and conformation, and can prevent the formation of the orderly crystal lattice necessary for structural analysis [1,2]. Overcoming this problem is not straightforward because of the potential importance of attached carbohydrate for protein solubility and its critical role in glycoprotein biosynthesis. In mammalian cells the correct folding and oligomerization of complex, multidomain proteins is controlled by N-glycosylation [3]. Reversible trimming of newly synthesized N-glycosylated polypeptides by glucosidase and glucosyltransferase enzymes controls their transient association with the two lectin chaperones calnexin and calreticulin [3]. Binding to calnexin and calreticulin slows down the rate of folding and prevents the occurrence of premature associations before all protein domains have been synthesized. This reversible process of glucosylation/lectin binding and deglucosylation/lectin release continues until the glycoprotein is correctly folded and assembled [3,4]. Chaperone-mediated glycoprotein folding, including the effects of selectively removing specific glycosylation sites [4], has been studied extensively with influenza virus haemagglutinin (HA) and has been investigated more recently with the human insulin receptor (hIR) [5].

The hIR is a multidomain, dimeric, membrane-bound glycoprotein composed of two α chains and two β chains, the latter having a single membrane-spanning sequence [6]. The receptor is initially synthesized as a single-chain proreceptor, which is glycosylated and proteolytically processed to α and β chains during transport to the cell surface [7–10]. Each monomer in the extracellular region comprises an α chain (residues 1–719 or 731 depending on the isoform [11]) and 194 residues of the β chain. Sequence analyses revealed that the ectodomain of each monomer contains seven domains: L1, Cys-rich, L2, three fibronectin type III (FnIII) modules and an insert domain of approx. 120–130 residues [12–19] predicted to be located in the C′–E loop [17] or the E–F loop [19,20] of the second FnIII domain. The dimer disulphide bonds are located in the first FnIII module and the insert domain [21].

The hIR is heavily glycosylated and is estimated to contain 58–64 kDa of carbohydrate [22]. Oligosaccharides of both the high-mannose and complex type are present, the latter containing additional fucose, *N*-acetylglucosamine, galactose and sialic acid residues [6,7,23,24]. The hIR has 18 potential sites for N-linked glycosylation, 14 on the α chain and 4 on the β chain, of which 16 have been confirmed as glycosylated (L. G. Sparrow, personal communication). O-linked glycosylation has been demonstrated only in the β subunit [23,25,26]. Other members of the insulin receptor family have fewer potential N-linked glycosylation sites, suggesting that not all sites are required for correct folding, assembly and function. As summarized in Figure 1, the IGF human insulin-like growth factor type 1 receptor (hIGF-1R) has 16 potential N-linked glycosylation sites [27], whereas the human insulin-receptor-related receptor (hIRR) has 11 sites [28].

Simultaneous mutation (Asn → Gln) of the four N-linked glycosylation sites (residues 742, 755, 893 and 906) in the β chain

Abbreviations used: CHO, Chinese hamster ovary; ER, endoplasmic reticulum; FnIII, fibronectin type III; HA, haemagglutinin; hIR, human insulin receptor; hIGF-1R, human insulin-like growth factor type 1 receptor; hIRR, human insulin-receptor-related receptor; mAb, monoclonal antibody.

[1] To whom correspondence should be addressed (e-mail colin.ward@hsn.csiro.au).

of the exon +11 isoform had no effect on hIR processing, intracellular transport or insulin binding but did have a deleterious effect on autophosphorylation and signal transduction [29]. In contrast, similar mutation of the four glycosylation sites (residues 16, 25, 78 and 111) in the L1 domain abolished proreceptor processing and intracellular transport to the plasma membrane [30]. However, glycosylation at all these sites was not required because single-site mutations at either residue 16 or 25 had little effect compared with the significant decrease in cell surface receptor levels when both residues 16 and 25 were mutated [31]. Similarly, glycosylation at either 397 or 418, but not at both sites, is required for normal receptor biosynthesis [32].

To understand the requirements of N-linked glycosylation during hIR biosynthesis, we have used site-directed mutagenesis to remove the N-linked glycosylation sites at 15 positions in various combinations. The effects of these mutations on proreceptor processing into α and β subunits, cell surface expression, insulin binding and receptor autophosphorylation were measured. Mutants of hIR with six (Δ6, $N^{16,337,418,730,743,881}Q$) or seven ($\Delta$7a, $S^{297}N/N^{16,337,418,730,743,881}Q$) sites removed could be generated that appeared normal by all criteria. These mutated proteins were expressed as soluble, secreted ectodomains in Chinese hamster ovary (CHO)-K1 cells and Lec8 cells [33] and the Δ6 ectodomain was produced in large-scale fermentation for structural analyses and crystallization screens. Atomic-level structural information is required to understand the molecular mechanisms by which the binding of insulin to its receptor initiates signal transduction.

EXPERIMENTAL

Mutagenesis

The DNA used in these studies was derived from a full-length hIR cDNA from plasmid peT [34], in which the 1.8 kbp *Aat*II fragment, which harbours exon 11, was exchanged for the equivalent fragment from an exon 11-minus partial hIR cDNA from plasmid pHIR/P12-1 [9]. Three fragments of hIR cDNA from this plasmid, peT/11$^-$, were introduced into M13mp18 [35] for mutagenesis: a 1.0 kbp *Eco*RI fragment, which included DNA encoding the N-terminal amino acid sequence from the signal peptide to amino acid residue 294; a 0.9 kbp *Eco*RI–*Bam*HI fragment encoding residues 295–599; and a 2.7 kbp *Bam*HI–*Xba*I fragment encoding the C-terminal sequence from residue 600. Oligonucleotide-directed mutagenesis of these fragments *in vitro* with the USB-T7 Gen™ *in vitro* mutagenesis kit was employed to remove 15 selected N-linked glycosylation sites by mutating asparagine residues 16, 78, 111, 215, 255, 337, 418, 514, 606, 624, 671, 730, 743 and 881 to glutamine and the serine residue at 297 to asparagine (see Figure 1). The mutation of S^{297} in the consensus site for N^{295} glycosylation was performed to avoid the destruction of an *Eco*RI site required for the later reinsertion of fragments. Clones incorporating the mutations were identified by colony hybridization [36] with ^{32}P-labelled mutagenic oligonucleotide as a probe; the mutations were confirmed by DNA sequence determination [37].

A vehicle for the mammalian cell expression of hIR cDNA with which the mutated fragments could be exchanged was prepared from the expression vector pEE14 (Celltech Ltd., Slough, Bucks., U.K.) [38] modified by the deletion of *Eco*RI and *Bam*HI restriction sites through fill-in and religation. The hIR cDNA for this construct was taken from plasmid peT/11$^-$ (described above), which has two *Eco*RI sites: one in an upstream polylinker sequence, the other in the hIR cDNA sequence. The site in the polylinker was deleted by partial *Eco*RI digestion, fill-in and religation to facilitate the subsequent exchange of fragments. The hIR cDNA from this plasmid, peT/11$^-$/Δ*Eco*RI, was inserted into the polylinker of the modified pEE14 expression vector as a *Hin*dIII–*Xba*I fragment. Mutated DNA was introduced into the hIR cDNA of this vehicle by the exchange of a 0.94 kbp *Not*I–*Eco*RI fragment (encoding residues -18 to 294 of insulin receptor), the 0.9 kbp *Eco*RI–*Bam*HI fragment and the 2.7 kbp *Bam*HI–*Xba*I fragment. The cell lines with different combinations of deglycosylation mutations are listed in Table 1 below.

Constructs for producing the soluble secreted ectodomain of the mutant receptor were made with an *Ssp*I cleavage site located 9 nt upstream of the encoded transmembrane region in hIR cDNA [8,9]. The presence of several *Ssp*I sites in plasmid pEE14 necessitated a three-way ligation involving (1) the larger *Xba*I–*Bam*HI fragment from the expression vehicle of mutant receptors (which included the entire pEE14 expression vector sequence with the encoded hIR sequence to residue 599), (2) a *Bam*HI–*Ssp*I fragment of hIR cDNA encoding residues 600–914 and harbouring mutations at residues 730, 743 and 881, and (3) a small synthetic oligonucleotide linker encoding an in-frame translation stop signal [22] to join the *Ssp*I and *Xba*I termini.

Transfection and screening

For transient transfection assays, 293T cells were grown in Dulbecco's modified Eagle's medium (Gibco BRL, Gaithersburg, MD, U.S.A.) plus 10% (v/v) foetal calf serum, to 50–80% confluence, and were then transfected with plasmid DNA with FuGENE (Roche Molecular Biochemicals) in accordance with the manufacturer's instructions. Cells were cultured for 2 days before serum starvation overnight and subsequent use.

Stable cell lines were prepared in CHO-K1 and Lec8 cells as follows. Cells were grown to between 50% and 80% confluence in minimum essential medium α medium (Gibco BRL) including 2 mM glutamine and 10% (v/v) foetal calf serum before transfection with DNA–liposome complexes prepared with Lipofectamine (Gibco BRL). After cell recovery and exchange of media to glutamine-free Glasgow's modified Eagle's medium (ICN Biomedicals, Costa Mesa, CA, U.S.A.) plus 10% (v/v) dialysed foetal calf serum, cells were selected with 25 μM methionine sulphoximine (Sigma). This inhibitor of glutamine synthase prevents the growth of cells not harbouring multiple copies of the glutamine synthase minigene from plasmid pEE14 [38]. Colonies (or supernatant for ectodomain constructs) were screened for protein expression by ELISA. Cell lines expressing a high level of receptor were selected by FACS and were cloned by limiting dilution. The ELISA employed anti-(insulin receptor) monoclonal antibody (mAb) 83.7 as the capture antibody and biotin-labelled mAb 83.14 for detection [39]. In FACS analysis, cells were treated with mAb 83.7 followed by FITC-labelled anti-mouse secondary antibody from sheep.

Metabolic labelling

Subconfluent cells were washed and incubated for 30 min in methionine/cysteine-free Dulbecco's modified Eagle's medium and then labelled by growth overnight in the presence of 5 μl (50 μCi) of methionine/cysteine Tran^{35}S-label (ICN Biomedicals). Cells were collected and solubilized by the method of Lammers et al. [40] and hIR from the lysate was immunoprecipitated with mAb 83.14 (4 μg) and Protein A–Sepharose (Sigma) slurry (20 μl). Immunoprecipitates were washed, boiled in Laemmli sample buffer under reducing conditions [41] and analysed by SDS/PAGE. Gels were fixed and soaked in Amplify

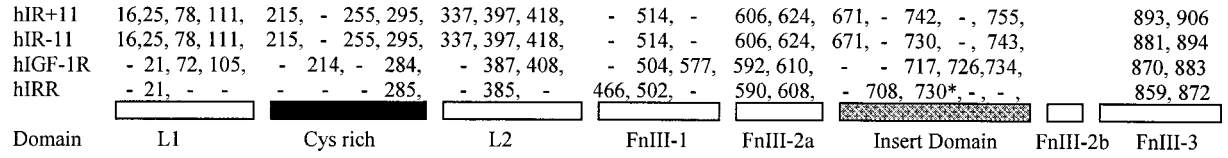

Figure 1 Distribution of potential N-linked glycosylation sites in hIR, hIGF-1R and hIRR ectodomains

Residue numbers of the potential N-linked glycosylation sites in hIR, hIGF-1R and hIRR are shown above the diagram of the structural modules that make up the hIR ectodomain. There are two isoforms of the hIR that differ in the presence or absence of 12 amino acid residues coded for by exon 11. The glycosylation site at 730 in hIRR (marked with an asterisk) occurs in a similar location to hIGF-1R 717 and hIR 730. This region of hIRR shows negligible sequence similarity to the other two receptors.

Table 1 Summary of glycosylation mutagenesis

Values for binding affinity are means ± S.E.M. Cell-surface values are relative to CHO.T cells.

			Effects			
Mutant type	Cell line	Mutation	Cell surface (%)	Processing	Binding affinity, K_d (M)	Autophosphorylation
Whole receptor	CHO.T	wild-type hIR	100	Normal	$(0.6 \pm 0.2) \times 10^{-10}$	Normal
	Δ2a	$N^{16,78}Q$	120	Normal	$(0.7 \pm 0.3) \times 10^{-10}$	Normal
	Δ2b	$N^{16,111}Q$	170	Normal	$(1.3 \pm 1.0) \times 10^{-10}$	Normal
	Δ2c	$N^{16,215}Q$	170	Normal	$(1.1 \pm 0.4) \times 10^{-10}$	Normal
	Δ2d	$N^{16,255}Q$	165	Normal	$(1.2 \pm 0.3) \times 10^{-10}$	Normal
	Δ3a	$N^{16,215,255}Q$	10	~ 4%*	Not detectable	†
	Δ3b	$S^{297}N$, $N^{337,418}Q$	95	Normal	$(1.0 \pm 0.3) \times 10^{-10}$	Normal
	Δ3c	$S^{297}N$, $N^{418,514}Q$	100	Normal	$(0.3 \pm 0.1) \times 10^{-10}$	Normal
	Δ2e	$N^{337,418}Q$	110	Normal	$(0.3 \pm 0.1) \times 10^{-10}$	Normal
	Δ3d	$N^{337,418,514}Q$	80	Normal	$(1.8 \pm 0.6) \times 10^{-10}$‡	Normal
	Δ3e	$N^{730,743,881}Q$	120	Normal	$(0.8 \pm 0.4) \times 10^{-10}$	Normal
	Δ4a	$N^{606,730,743,881}Q$	190	Normal	$(0.8 \pm 0.1) \times 10^{-10}$	Normal
	Δ4b	$N^{624,730,743,881}Q$	159	Normal	$(0.8 \pm 0.2) \times 10^{-10}$	Constitutively active
	Δ4c	$N^{671,730,743,881}Q$	200	Normal	$(1.2 \pm 0.3) \times 10^{-10}$	Normal
	Δ6	$N^{16,337,418,730,743,881}Q$	170	Normal	$(0.4 \pm 0.1) \times 10^{-10}$	Normal
	Δ7a	$S^{297}N$, $N^{16,337,418,730,743,881}Q$	100	Normal	$(1.1 \pm 0.7) \times 10^{-10}$	Normal
	Δ7b	$N^{16,337,418,514,730,743,881}Q$	60	0–25%§	$(1.1 \pm 0.1) \times 10^{-10}$	†
Ectodomain	hIR ecto	wild-type hIR ecto			$(2.1 \pm 0.2) \times 10^{-8}$ (CHO-K1); $(1.2 \pm 0.2) \times 10^{-8}$ (Lec8)	
	Δ6 ecto	$N^{16,337,418,730,743,881}Q$			$(0.4 \pm 0.1) \times 10^{-8}$ (CHO-K1); $(0.3 \pm 0.1 \times 10^{-8}$ (Lec8)	
	Δ7a ecto	$S^{297}N$, $N^{16,337,418,730,743,881}Q$			$(0.3 \pm 0.1) \times 10^{-8}$ (CHOK-1); $(0.3 \pm 0.1) \times 10^{-8}$ (Lec8)	

* Transient expression in 293T cells.
† The small proportion of receptor correctly processed showed normal autophosphorylation.
‡ Most extreme value ($P = 0.06$).
§ 0% in 293T cells (transients); 15–25% in CHO-K1 cells (stable cell lines).

(Amersham, Little Chalfont, Bucks., UK) before being dried and subjected to autoradiography. X-ray films were scanned with a Gel-Pro Analyser, version 3 (Media Cybernetics, Silver Spring, MD, U.S.A.).

Autophosphorylation

A simple immunoblotting assay for comparing the relative levels of receptor autophosphorylation was employed with stable CHO cell lines and transiently transfected 293T cells. Subconfluent cells were deprived of serum overnight and then incubated in the presence or absence of insulin (100 nM) for 10 min. Receptor from cells was prepared as above in the presence of Na_3VO_4 (1 mM) to inhibit phosphatases, then fractionated by SDS/PAGE and transferred to nitrocellulose membrane. Phosphorylated β subunit was detected by probing with anti-phosphotyrosine antibody (PY 20) conjugated to horseradish peroxidase (Santa Cruz Biotechnology, Santa Cruz, CA, U.S.A.), followed by SuperSignal™ chemiluminescent substrate (Pierce, Rockford, IL, U.S.A.) and exposure to Hyperfilm™ (Amersham). Films were scanned with a Gel-Pro Analyser, version 3 (Media Cybernetics). To demonstrate comparable receptor levels in assays, the membrane was stripped of antibody and reprobed with an antibody against hIR β chain (mAb CT-1), followed by an anti-(mouse IgG) antibody conjugated to horseradish peroxidase for detection (Santa Cruz Biotechnology).

Insulin binding

To assess the affinity for insulin of mutagenized receptors, the binding of ^{125}I-insulin (Dupont NEN, Boston, MA, U.S.A.) was examined over a range of unlabelled insulin concentrations in a

solid-phase assay with mAb immobilized on microtitre plates to capture detergent-released insulin receptor or soluble, secreted ectodomain [42]. Insulin bound to receptor was determined, after extensive washing, by counting γ radioactivity. Results were collated and analysed with the LIGAND program [43] and plotted on Scatchard coordinates [44]. Binding constants represent the means for three experimental determinations for mutants and eight for the CHO.T control cell line, which overexpresses wild-type hIR [34]. A statistical comparison of groups of experimental values was performed with Student's t test.

Ectodomain purification and characterization

Ectodomain from large-scale fermentation of Lec8 cells was recovered from medium as a soluble protein by affinity chromatography on a bis-(t-butoxycarbonyl)insulin column and further purified to remove oligomers and cleavage products by gel filtration on a Superdex 200 HR 10/30 column (Pharmacia), essentially as described previously [16,22]. The molecular mass of ectodomain from Lec8 cells was determined by ultracentrifugation, assuming the same partial specific volumes of carbohydrate and protein as used previously for the molecular mass determination of CHO-K1-derived ectodomain [22]. Ectodomain proteins were compared before and after treatment with neuraminidase by SDS/PAGE and by isoelectric focusing in Novex (San Diego, CA, U.S.A.) pH 3–7 polyacrylamide gel. Gels were fixed, stained and destained in accordance with the manufacturer's instructions. Neuraminidase from avian N9 influenza virus [22] was used at an enzyme-to-substrate ratio of 1:100 in phosphate buffer, pH 7.0, at 37 °C for 2 h.

RESULTS

Whole hIR mutants

The locations of the potential N-linked glycosylation sites are shown schematically in Figure 1. Of the 18 sites in hIR, 15 were mutated in different combinations. The exceptions were the sites at 25, 397 and 894, which have previously been shown to be important for hIR biosynthesis or function [26,31,32]. These three sites, along with five others, are conserved in hIGF-1R and hIRR (Figure 1).

The 16 stable CHO-K1 cell lines expressing intact hIR with various combinations of glycosylation sites removed are listed in Table 1. Cell-surface expression was monitored by FACS analysis with mAb 83.7 [39]. All except one of the stable cell lines showed increases in fluorescence of more than 18-fold that of the parental CHO-K1 cell line (Figure 2) and comparable with that of the CHO.T cell line (Table 1), which produces more than 250000 insulin receptors per cell [34]. The one exception was the Δ3a mutant ($N^{16,215,255}Q$), which was poorly transported to the cell surface. The increase in fluorescence for this cell line was approx. 3.5-fold (Figure 2).

Analysis of mutant receptors by metabolic labelling and SDS/PAGE showed the characteristic pattern of proreceptor, α chain and β chain consistent with normal receptor processing, for all cell lines except Δ7b (Table 1, Figure 3) and Δ3a (results not shown). Both produced mainly uncleaved proreceptor (Figures 3 and 4), despite the large difference in cell-surface expression levels discussed above. The amounts of correctly cleaved Δ3a and Δ7b, after transient expression in 293T cells, were 4% and negligible respectively, as judged by densitometric scanning of Western blots (Figure 4B). The amount of correctly cleaved Δ7b when expressed in CHO-K1 cells ranged from 15% to 25% as judged by densitometric scanning of autoradiographs

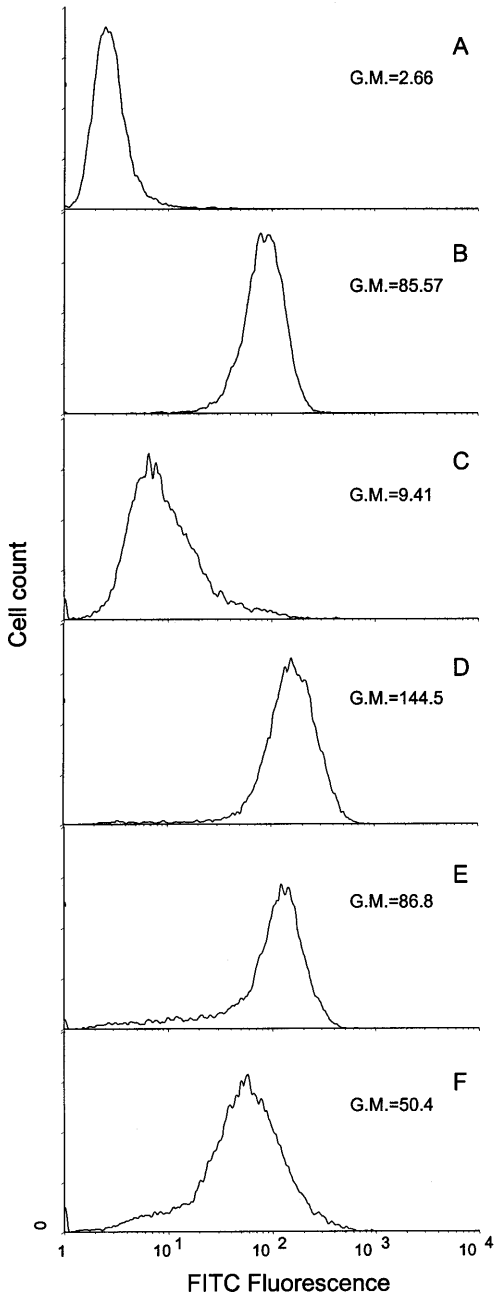

Figure 2 Flow-cytometric analysis of CHO-K1 cells overexpressing wild-type or deglycosylation mutants of insulin receptor

Cells were treated with anti-hIR mAb 83.7 followed by fluorescein isothiocyanate (FITC)-labelled, sheep anti-mouse secondary antibody. Flow cytometer excitation was with a 488 nm argon-ion laser and FITC emission was analysed at 525 nm. Abbreviation: G.M., geometric mean. (**A**) CHO-K1; (**B**) CHO.T (i.e. wild-type hIR); (**C**) mutant Δ3a ($N^{16,215,255}Q$); (**D**) mutant Δ6 ($N^{16,337,418,730,743,881}Q$); (**E**) mutant Δ7a ($S^{297}N$, $N^{16,337,418,730,743,881}Q$); (**F**) mutant Δ7b ($N^{16,337,418,514,730,743,881}Q$).

of metabolically labelled receptor (Figure 3). As expected, the α and β chains of mutant receptors showed smaller apparent molecular masses than wild-type receptor subunits, particularly for the higher-order mutants (Figure 3).

In insulin binding studies, most of the 16 mutated receptors bound insulin with a high affinity that did not differ significantly from that of the wild-type receptor expressed by the CHO.T cell

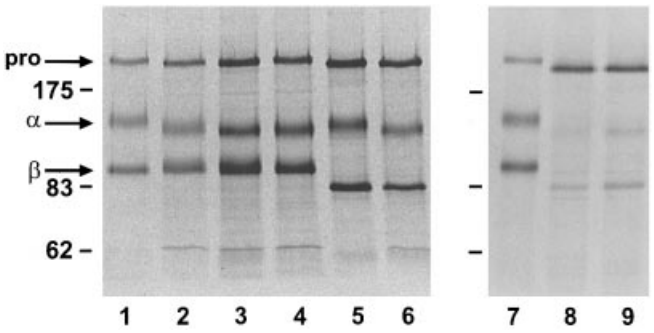

Figure 3 SDS/PAGE analysis of reduced, metabolically labelled insulin receptor mutants expressed in CHO-K1 cells

Cells were metabolically labelled with [^{35}S]cysteine/methionine. The insulin receptors were solubilized and immunoprecipitated with mAb 83.14 and Protein A–Sepharose as described in the Materials and methods section. Immunoprecipitates were washed, boiled in Laemmli sample buffer under reducing conditions and analysed by SDS/PAGE [6% (w/v) gel]. Gels were fixed and soaked in Amplify before being dried and subjected to autoradiography. Lane 1, CHO.T (i.e. wild-type hIR); lane 2, mutant Δ3d ($N^{337,418,514}Q$); lane 3, mutant Δ3b ($S^{297}N$, $N^{337,418}Q$); lane 4, mutant Δ3c ($S^{297}N$, $N^{418,514}Q$); lane 5, mutant Δ6 ($N^{16,337,418,730,743,881}Q$); lane 6, mutant Δ7a ($S^{297}N$, $N^{16,337,418,730,743,881}Q$); lane 7, CHO.T; lanes 8 and 9, mutant Δ7b ($N^{16,337,418,514,730,743,881}Q$, two clones). The migration positions of molecular mass markers (in kDa) are indicated at the left of each gel. Proreceptor (pro), α subunit and β subunit are indicated at the left of lane 1.

line (Table 1). The exceptions were mutant Δ3d, which exhibited a marginally lower binding affinity ($P = 0.06$), and mutant Δ3a, which showed negligible insulin binding owing to the low level of surface expression of processed receptor (Figure 2). Although stable cell lines of mutant Δ7b bound sufficient insulin to determine the binding affinity (Table 1), 293T cells transiently transfected with Δ7b showed negligible binding relative to cells transfected with wild-type hIR. This suggests that only the small amount of fully processed Δ7b receptor in the stable cell lines could bind insulin. All mutant receptors, which bound sufficient insulin for data collection (i.e. all except Δ3a), showed concave curvilinearity in Scatchard plots at supraphysiological concentrations of insulin [42].

In all mutant cell lines except Δ3a, Δ4b and Δ7b, stimulation of receptor autophosphorylation with insulin was comparable with that of wild-type receptor from CHO.T as judged by β-chain phosphorylation (Table 1). Photographic exposure times, which detected a very low signal in basal level autophosphorylation (1.9–2.7% of the insulin-stimulated signal), showed strong signals after stimulation with insulin (Figure 4). The Δ4b mutant was constitutively active, showing a high basal level of activity that did not increase after stimulation with insulin (Figure 4). Although the levels of processed receptor on the cell surface of mutant Δ3a were low, the receptor nevertheless seemed to display normal insulin-induced autophosphorylation (Figure 4). The Δ7b mutant, which was expressed at high levels on the cell surface, displayed negligible proreceptor processing or insulin-induced autophosphorylation signal (Figure 4). When longer exposure times were used, autophosphorylation of Δ7b was restricted to the small amount of processed receptor.

Secreted hIR ectodomains

The Δ6 and Δ7a mutations were incorporated into constructs for expression as soluble, secreted ectodomains in both CHO-K1 cells and the Lec8 mutant of CHO-K1 cells, which produce N-linked oligosaccharides lacking terminal galactose and *N*-acetylneuraminic acid residues. Wild-type ectodomain produced in Lec8 cells showed normal processing into α and truncated β subunits (β′) with decreased apparent molecular masses on SDS/PAGE relative to the corresponding ectodomain produced in CHO-K1 cells (Figure 5, lanes 1–3 and 4–6). Analytical ultracentrifugation of purified wild-type ectodomain indicated a decrease in molecular mass of ectodomain from 270 kDa in CHO-K1 cells [22] to 240 kDa in Lec8 cells and a further decrease to 230 kDa for the ectodomain of mutant Δ6.

The Lec8-expressed hIR ectodomain showed little difference in insulin binding relative to the corresponding ectodomain from CHO-K1 cells (Table 1); all ectodomain preparations had linear Scatchard plots for insulin binding. Insulin affinity was higher ($P < 0.05$) for the ectodomain of glycosylation-site mutants than for unmodified ectodomain (Table 1).

Large-scale fermentations of Lec8 cells yielded 2–3 mg/l of ectodomain from wild-type receptor or from the mutant Δ6 as estimated by amino acid analysis, with 90% of the product recovered by affinity chromatography [16,22] as estimated by ELISA. A comparison of charge heterogeneity between these products and the ectodomain from CHO-K1 cells was made by

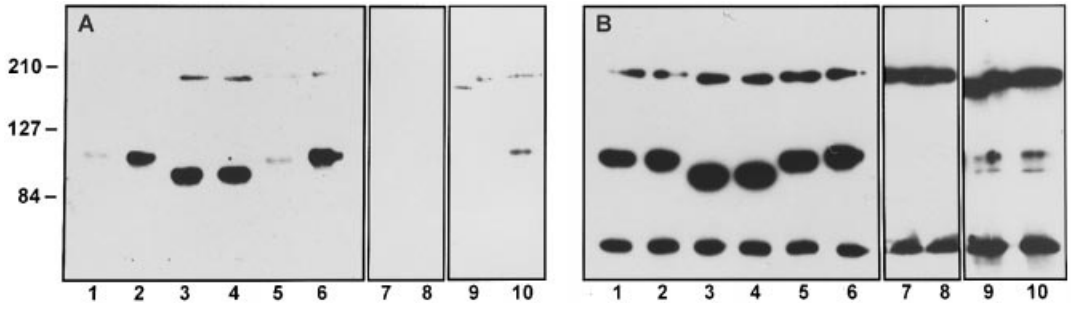

Figure 4 Detection of autophosphorylation by immunoblotting

Insulin receptors from transiently transfected 293T cells were fractionated by SDS/PAGE [7.5% (w/v) gel] and transferred to nitrocellulose membrane. Phosphorylated β subunit was detected by probing with anti-phosphotyrosine antibody. The membrane was then stripped of antibody against and reprobed with an antibody against hIR β chain (mAb CT-1). (**A**) Anti-phosphotyrosine antibody, PY 20; (**B**) anti-(β chain) antibody, mAb CT1. Lanes 1 and 2, CHO.T (i.e. wild type); lanes 3 and 4, mutant Δ4b ($N^{624,730,743,881}Q$); lanes 5 and 6, mutant Δ2c ($N^{16,215}Q$), representative of the mutants showing normal responses; lanes 7 and 8, mutant Δ7b ($N^{16,337,418,514,730,743,881}Q$); lanes 9 and 10, mutant Δ3a ($N^{16,215,255}Q$). Lanes 1, 3, 5, 7 and 9 were non-stimulated cells; lanes 2, 4, 6, 8 and 10 were insulin-stimulated cells. The 55 kDa band in (**B**) resulted from detection of the immunoprecipitating antibody heavy chain, because a secondary anti-mouse IgG antibody was used in detection of mAb CT1.

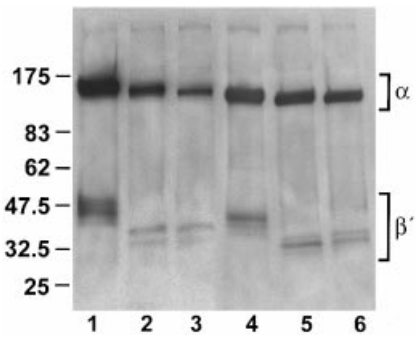

Figure 5 SDS/PAGE analysis of metabolically labelled insulin receptor ectodomain expressed in CHO-K1 or Lec8 cells

Cells were metabolically labelled with [^{35}S]cysteine/methionine. Protein from conditioned medium was immunoprecipitated with mAb 83.14 and Protein A–Sepharose as described in the Materials and methods section. Immunoprecipitates were washed, boiled in Laemmli sample buffer under reducing conditions and analysed by SDS/PAGE [4–15% (w/v) gradient gel]. Gels were fixed and soaked in Amplify before being dried and subjected to autoradiography. The cell line was CHO-K1 in lanes 1, 2 and 3, and Lec8 in lanes 4, 5 and 6. Lanes 1 and 4, wild-type ectodomain; lanes 2 and 5, mutant Δ6 ($N^{16,337,418,730,743,881}Q$) ectodomain; lanes 3 and 6, mutant Δ7a ($S^{297}N$, $N^{16,337,418,730,743,881}Q$) ectodomain. The migration positions of molecular mass markers (in kDa) are shown at the left, and α subunit and β′ subunit at the right.

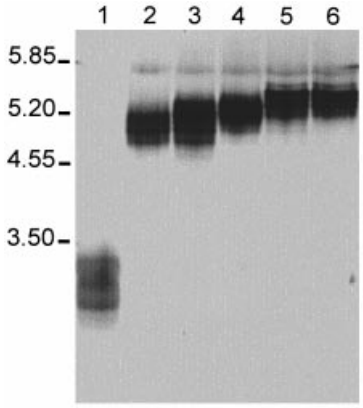

Figure 6 Isoelectric focusing of ectodomain preparations in polyacrylamide gel (5%, w/w)

Insulin receptor ectodomain protein was produced by large-scale fermentation of transfected CHO-K1 or Lec8 cells and purified by insulin-affinity chromatography and gel filtration as described in the Materials and methods section. Aliquots (5–10 μg in 15 μl) were mixed with 15 μl of sample buffer and subjected to isoelectric focusing in pH 3–7 polyacrylamide gels. Where indicated, protein samples were treated with neuraminidase from avian N9 influenza virus. Lane 1, wild-type ectodomain (CHO-K1); lane 2, neuraminidase-treated wild-type ectodomain (CHO-K1); lane 3, wild-type ectodomain (Lec8); lane 4, neuraminidase-treated wild-type ectodomain (Lec8); lane 5, mutant Δ6 ($N^{16,337,418,730,743,881}Q$) ectodomain (Lec8); lane 6, neuraminidase-treated mutant Δ6 ($N^{16,337,418,730,743,881}Q$) ectodomain (Lec8). The positions and pH values of marker proteins are indicated.

isoelectric focusing (Figure 6). Wild-type ectodomain from CHO-K1 cells revealed a pattern of multiple, closely spaced isoforms ranging from pI 4.0 to 4.5, considerably more acidic than the pI estimated from the amino acid composition, reflecting the presence of variable end-capped sialylation expected in CHO-K1 cells. Isoelectric focusing of Lec8-derived, wild-type ectodomain showed isoforms of higher pH range from pI 5.25 to 5.6. Neuraminidase treatment of the wild-type ectodomain produced in CHO-K1 cells transposed the pI range to higher pH values, similar to that seen with the Lec8-derived product. The Δ6 mutant from Lec8 cells produced isoforms over a narrower range, from pI 5.45 to 5.65. Treatment with neuraminidase produced no detectable change in this pattern (Figure 6).

DISCUSSION

Studies aimed at elucidating the steps involved in the expression, folding and assembly of the mature insulin receptor homodimer have been reviewed recently [45]. Glycosylation is critical for insulin receptor biosynthesis. Inhibition of N-linked glycosylation by tunicamycin leads to the intracellular accumulation of aglyco-proreceptors, which fail to form correctly assembled tertiary and quaternary structures [46]. The lectin chaperones calnexin and calreticulin, together with the heat-shock protein 70 analogue BiP, control the folding of proteins in the endoplasmic reticulum (ER) [3]. Calreticulin, and to a smaller extent calnexin, have been shown to associate with both the early monomeric and late monomeric proreceptor species of insulin receptor but not with the insulin receptor dimers [5]. This suggests that once the insulin receptor monomers have been correctly folded these lectin chaperones no longer bind, permitting receptor dimerization followed by export from the ER. When calnexin and calreticulin binding is blocked by castanospermine, insulin receptor dimerization is accelerated but the receptor protein is retained in the ER through interactions with BiP until it is correctly folded and transported to the trans-Golgi [5]. The ability to form functional receptors in the absence of ER lectin binding but not in the absence of glycosylation indicates that N-linked carbohydrate also functions to enhance the solubility of insulin receptor and to counteract aggregate formation [47].

In this study we have investigated the effects of removing N-linked glycosylation sites from various regions of the hIR. The effects of these mutations are summarized in Table 1 and the comparative data for other glycosylation site mutations are summarized in Table 2. These studies indicate that there are many redundancies in hIR glycosylation sites and that every site can be mutated individually without detriment to cell-surface expression, receptor processing and ligand binding. When combinations of sites are examined, it seems that major domains of the receptor, particularly those closer to the N-terminus (i.e. L1, Cys-rich, L2), require at least one intact glycosylation site to ensure correct folding and processing. In the studies of the effects of the removal of different glycosylation sites on the folding and assembly of influenza virus HA, it was concluded that specific glycosylation sites, particularly those that are distal to the membrane surface, are important to allow these protein domains to be sequestered by calreticulin and calnexin until polypeptide synthesis is complete [4]. These distal sites in HA were bound preferentially by calreticulin, which, unlike calnexin, is not membrane-bound. Interestingly, much more of the hIR proreceptor in the ER was found to be associated with calreticulin than with calnexin [5].

Removal of the four glycosylation sites in the N-terminal L1 domain (at residues 16, 25, 78 and 111) resulted in the complete retention of proreceptor in the ER and no proreceptor processing [30,31,48]. The mutant proreceptor was a dimer and could bind insulin, but failed to show insulin-induced kinase activity *in vitro* [48]. Of the four sites, that at residue 25, which is conserved in all three members of the insulin receptor family (Figure 1), seems to be the most important. The double mutant at 16 and 25 and the triple mutant 25, 78 and 111 were severely compromised in terms of processing and cell-surface expression (Table 2), although the receptor that is processed binds and autophosphorylates normally [31]. The triple mutant 16, 78 and 111 and the double

Table 2 Summary of previous glycosylation mutagenesis

Cell-surface values are relative to CHO.T cells. Abbreviation: n.d., not determined.

Cell line	Mutation	Cell surface (%)	Processing	Binding affinity	Autophosphorylation	Reference
α^{1}	$N^{16}Q$	100	Near normal	Normal	Normal	[31]
α^{2}	$N^{25}Q$	100	Marginally decreased	Normal	Normal	[31]
$\alpha^{1,2}$	$N^{16,25}Q$	~ 9	Greatly decreased	Normal	Normal	[31]
$\alpha^{3,4}$	$N^{78,111}Q$	~ 36	Decreased	Normal	Normal	[31]
$\alpha^{1,3,4}$	$N^{16,78,111}Q$	~ 27	Decreased	Normal	Normal	[31]
$\alpha^{2,3,4}$	$N^{25,78,111}Q$	~ 9	Greatly decreased	Normal	Normal	[31]
$\alpha^{1,2,3,4}$	$N^{16,25,78,111}Q$	0	None	n.d.	n.d.	[31]
1234		0	None	n.d.	n.d.	[30]
4NQ		0	None	+ve binding by lysates	Defective	[48]
Q397	$N^{397}Q$	100	Normal	Normal	Normal	[32]
Q419	$N^{418}Q$	100	Normal	Normal	Normal	[32]
Q-D	$N^{397,418}Q$	0	None, degraded	Not detectable	Not detectable	[32]
βN^{1}	$N^{742}Q$	100	Normal	Normal	Normal	[26]
βN^{2}	$N^{755}Q$	100	Normal	Normal	Normal	[26]
βN^{12}	$N^{742,755}Q$	100	Normal	Normal	Normal	[26]
βN^{3}	$N^{893}Q$	100	Normal	Normal	61%	[26]
βN^{4}	$N^{906}Q$	100	Normal	Normal	20% basal up	[26]
βN^{34}	$N^{893,906}Q$	100	Normal	Normal	20% basal up	[26]
βN^{1234}	$N^{742,755,893,906}Q$	100	Normal	Normal	Impaired	[26,29]

mutant 78 and 111 were not as severely affected [31]. The two L1-domain double mutants 16 and 78 (Δ2a) and 16 and 111 (Δ2b) examined in this study were processed normally (Table 1).

In the Cys-rich domain, none of the three sites (residues 215, 255 and 295) seem to be critical individually. The double mutants Δ2c (16 + 215) and Δ2d (16 + 255) were normal, as were the triple and higher-order mutants Δ3b, Δ3c and Δ7a, which lacked the conserved site at residue 295 (Table 1). The triple mutant Δ3a (16 + 215 + 255), from which the first two sites in the Cys-rich domain were removed along with residue 16, was poorly transported to the cell surface and little processed receptor was produced. The three-dimensional structure of the L1–Cys-rich–L2 region of the IGF-1R shows that residues 215 and 255 are located in a region of the Cys-rich domain that is in intimate contact with the L1 domain [15]. It seems that at least one N-linked oligosaccharide moiety is required in this region of the receptor for efficient folding to take place. Although there was insufficient Δ3a receptor to measure insulin binding directly, indirect evidence for insulin binding (by the small amount of processed receptor) came from the observation of insulin-induced autophosphorylation (Figure 4A).

There are three glycosylation sites in the L2 domain of the hIR (337, 397 and 418), one of which (residue 397) is conserved in hIGF-1R and hIRR (Figure 1). The simultaneous removal of two of these sites, residues 397 and 418, has been shown to affect receptor biosynthesis severely, whereas the individual mutation of either of these sites was without detrimental effect [32], as summarized in Table 2. The three-dimensional structure of the L1–Cys-rich–L2 domain fragment of hIGF-1R suggests, by homology, that both of these residues are located on the same face of the hIR L2 domain [15]. In the present study we have retained the site at residue 397 and shown that mutants lacking both 337 and 418 (Δ2e) are normal, as are the higher-order mutants Δ3b, Δ3d, Δ6 and Δ7a, which also lack this pair of L2 glycosylation sites (Table 1).

The single N-linked site (residue 514) in the first FnIII domain of the hIR is predicted to lie in the C–C′ loop at the base of this module [17–19]. Of the mutants lacking this site, mutant Δ3c seemed to be normal, whereas mutant Δ3d seemed normal except for a marginally lower insulin binding affinity (Table 1). This lower insulin binding affinity might be related to the fact that the three glycosylation sites (residues 337, 418 and 514) are located within a region (residues 325–524) that has been suggested to be a major determinant of high-affinity insulin binding [49]. Labelled insulin has been shown to associate with receptor sequence in this region [50]. The higher-order mutant Δ7b, which also included the 514 mutation, was not cleaved into α and β subunits, in contrast with mutants Δ6 and Δ7a, with which Δ7b shared six mutations (residues 16, 337, 418, 730, 743 and 881).

The four N-linked glycans of the β chain (at residues 742, 755, 893 and 906 in the exon 11^{+} isoform) can be removed simultaneously without affecting proreceptor processing, surface expression or insulin binding [29]. However, this mutant was defective in autophosphorylation and kinase activity and was unable to transduce the signals for glycogen or DNA synthesis [26,29]. Analysis of single-site and double-site mutations established that this signalling defect was caused predominantly by the mutation at residue 906, although removal of the site at N^{893} also depressed kinase activity by 40% [26,29]. In our studies with the exon 11^{-} isoform, removal of the first three N-glycosylation sites in the β chain had no effect on cell-surface expression, processing, insulin binding or autophosphorylation. These three mutations could be combined with removal of the site at either 606 (mutant Δ4a) or 671 (mutant Δ4c) or the multiple mutations at 16, 337, 418 (mutant Δ6) or 16, 295, 337, 418 (mutant Δ7a), without significantly affecting cell-surface expression, processing, insulin binding or autophosphorylation (Table 1). In contrast, the quadruple mutant Δ4b (sites 624, 730, 742, 881) showed normal processing and ligand binding, but was constitutively active as judged by autophosphorylation.

In this study we have expanded on previous results and have shown that for hIR, six or seven (39%) of the potential N-linked glycosylation sites can be removed without apparent detriment to surface expression, processing and insulin binding. Potential for further decrease in the number of sites might exist provided that the carbohydrate remaining can fulfil all functions required in the cell, and solubility is not compromised at the high protein concentrations required for crystallization. Among the other

remaining sites, residues 255 and 671 have no equivalent counterparts in either hIRR or hIGF-1R, suggesting that these sites might be suitable candidates for the more extensive elimination of glycosylation sites from hIR.

One of the major factors affecting the successful crystallization of proteins is the extent and heterogeneity of glycosylation [1,2]. The ectodomain of the insulin receptor has been produced previously as a soluble secreted protein in CHO-K1 cells and shown to contain 58–64 kDa of attached carbohydrate on the basis of a calculated apoprotein molecular mass of 209 kDa [22]. To decrease charge heterogeneity from partial sialylation and to lower oligosaccharide content, the production of ectodomain was examined in the Lec8 mutant CHO-K1 cell line, which has a defect in glycosylation [33]. Ultracentrifugation showed that the amount of attached carbohydrate on the Lec8-produced hIR ectodomain had been decreased to 30–32 kDa [16]. The carbohydrate content of ectodomain in the Δ6 mutant produced in Lec8 cells had been further decreased to 20–22 kDa, which is approximately one-third of the level present in the wild-type ectodomain expressed in the CHO-K1 cell line. This residual carbohydrate represents approx. 10% of the molecular mass of ectodomain, a level accordant with those of glycoproteins whose structures have been determined by X-ray diffraction. Ectodomain from this Δ6 mutant has not been compromised in biosynthesis or insulin binding relative to unmodified ectodomain and remains soluble at high protein concentration. It offers the possibility of a protein that might be more amenable to crystallization and diffraction studies than the wild-type ectodomain.

We thank Professor W. Rutter for supplying both the CHO.T cell line and plasmid peT harbouring hIR cDNA, Professor K. Siddle for supplying monoclonal cell lines producing anti-insulin-receptor antibodies, Dr G. Lovrecz for bulk fermentation, Dr G. Howlett for analytical ultracentrifugation, Dr Tim Adams for technical advice, and Ms A. Verkuylen for assistance with cell culture. Financial support was provided under the Generic Technology component of the Industry Research and Development Act 1986 and from Biota Diabetes Pty Ltd.

REFERENCES

1 Hendrickson, W. A. (1996) Production of crystallizable fragments of membrane proteins. J. Bioenerg. Biomembr. **28**, 35–40
2 Wyss, D. F. and Wagner, G. (1996) The structural role of sugars in glycoproteins. Curr. Opin. Biotechnol. **7**, 409–416
3 Trombetta, E. S. and Helenius, A. (1990) Lectins as chaperones in glycoprotein folding. Curr. Opin. Struct. Biol. **8**, 587–592
4 Hebert, D. N., Zhang, J.-X., Chen, W., Foellmer, B. and Helenius, A. (1997) The number and location of glycans on influenza hemagglutinin determine folding and association with calnexin and calreticulin. J. Cell. Biol. **139**, 613–623
5 Bass, J., Chiu, G., Argon, Y. and Steiner, D. F. (1998) Folding of insulin receptor monomers is facilitated by the molecular chaperones calnexin and calreticulin and impaired by rapid dimerization. J. Cell Biol. **141**, 637–646
6 Hedo, J. A. and Gorden, P. (1985) Biosynthesis of the insulin receptor. Horm. Metab. Res. **17**, 487–490
7 Hedo, J. A., Kahn, C. R., Hayashi, M., Yamada, K. M. and Kasuga, M. (1983) Biosynthesis and glycosylation of the insulin receptor. Evidence for a single polypeptide precursor of the two major subunits. J. Biol. Chem. **258**, 10020–10026
8 Ebina, Y., Ellis, L., Jarnagin, K., Edery, M., Graf, L., Clauser, E., Ou, J., Maslarz, F., Kan, Y. W., Goldfine, I. D. et al. (1985) The human insulin receptor cDNA: the structural basis for hormone-activated transmembrane signalling. Cell **40**, 747–758
9 Ullrich, A., Bell, J. R., Chen, E. Y., Herrera, R., Petruzeli, L. M., Dul, T. J., Gray, A., Coussens, L., Liao, Y.-C., Tsubokowa, M. et al. (1985) Human insulin receptor and its relationship to the tyrosine kinase family of oncogenes. Nature (London) **313**, 756–761
10 Ronnett, G. V., Knutson, V. P., Kohanski, R. A., Simpson, T. L. and Lane, M. D. (1984) Role of glycosylation in the processing of newly translated insulin proreceptor in 3T3–L1 adipocytes. J. Biol. Chem. **259**, 4566–4575
11 Seino, S., Seino, M., Nishi, S. and Bell, G. I. (1989) Structure of the human insulin receptor gene and characterization of its promoter. Proc. Natl. Acad. Sci. U.S.A. **86**, 114–118
12 Bajaj, M., Waterfield, M. D., Schlessinger, J., Taylor, W. R. and Blundell, T. (1987) On the tertiary structure of the extracellular domains of the epidermal growth factor and insulin receptors. Biochim. Biophys. Acta **916**, 220–226
13 O'Bryan, J. P., Frye, R. A., Cogswell, P. C., Neubauer, Z., Kitch, B., Prokop, C., Espinosa III, R., Le Beau, M. M., Earp, H. S. and Liu, E. T. (1991) *Axl*, a transforming gene isolated from primary human myeloid leukemia cells, encodes a novel receptor tyrosine kinase. Mol. Cell. Biol. **11**, 5016–5031
14 Ward, C. W., Hoyne, P. A. and Flegg, R. H. (1995) Insulin and epidermal growth factor receptors contain the cysteine repeat motif found in the tumor necrosis factor receptor. Proteins Struct. Funct. Genet. **22**, 141–153
15 Garrett, T. P. J., McKern, N. M., Lou, M., Frenkel, M. J., Bentley, J. D., Lovrecz, G. O., Elleman, T. C., Cosgrove, L. J. and Ward, C. W. (1998) Crystal structure of the first three domains of the type-1 insulin-like growth factor receptor. Nature (London) **394**, 395–399
16 Tulloch, P. A., Lawrence, L. J., McKern, N. M., Robinson, C. P., Bentley, J. D., Cosgrove, L., Ivancic, N., Lovrecz, G. O., Siddle, K. and Ward, C. W. (1999) Single-molecule imaging of human insulin receptor ectodomain and its Fab complexes. J. Struct. Biol. **125**, 11–18
17 Mulhern, T. D., Booker, G. W. and Cosgrove, L. (1998) A third fibronectin type-III domain in the insulin-family receptors. Trends Biochem. Sci. **23**, 465–466
18 Marino-Buslje, C., Mizuguchi, K., Siddle, K. and Blundell, T. L. (1998) A third fibronectin type III domain in the extracellular region of the insulin receptor family. FEBS Lett. **441**, 331–336
19 Ward, C. W. (1999) Members of the insulin receptor family contain three fibronectin type III domains. Growth Factors **16**, 315–322
20 Schaefer, E. M., Erickson, H. P., Federwisch, M., Wollmer, A. and Ellis, L. (1992) Structural organization of the human insulin receptor ectodomain. J. Biol. Chem. **267**, 23393–23402
21 Sparrow, L. G., McKern, N. M., Gorman, J. J., Strike, P. M., Robinson, C. P., Bentley, J. D. and Ward, C. W. (1997) The disulfide bonds in the C-terminal domains of the human insulin receptor ectodomain. J. Biol. Chem. **272**, 29460–29467
22 Cosgrove, L., Lovrecz, G. O., Verkuylen, A., Cavaleri, L., Black, L. A., Bentley, J. D., Howlett, G. J., Gray, P. P., Ward, C. W. and McKern, N. M. (1995) Purification and properties of insulin receptor ectodomain from large-scale mammalian cell culture. Protein Express. Purif. **6**, 789–798
23 Herzberg, V. L., Grigorescu, F., Edge, A. S. B., Sprio, R. G. and Kahn, C.R (1985) Characterization of insulin receptor carbohydrate by comparison of chemical and enzymatic deglycosylation. Biochem. Biophys. Res. Commun. **129**, 789–796
24 Hedo, J. A., Kasuga, M., Van Obberghen, E., Roth, J. and Kahn, C. R. (1981) Direct demonstration of glycosylation of insulin receptor subunits by biosynthetic and external labeling: evidence for heterogeneity. Proc. Natl. Acad. Sci. U.S.A. **78**, 4791–4795
25 Collier, E. and Gorden, P. (1991) O-linked oligosaccharides on insulin receptor. Diabetes **40**, 197–203
26 Leconte, I., Carpentier, J. L. and Clauser, E. (1994) The functions of the human insulin receptor are affected in different ways by mutation of each of the four N-glycosylation sites in the beta subunit. J. Biol. Chem. **269**, 18062–18071
27 Ullrich, A., Gray, A., Tam, A. W., Yang-Feng, T., Tsubokawa, M., Collins, C., Henzel, W., Le Bon, T., Kathuria, S., Chen, E. et al. (1986) Insulin-like growth factor 1 receptor primary structure: comparison with insulin receptor suggests structural determinants that define functional specificity. EMBO J. **5**, 2503–2512
28 Shier, P. and Watt, V. M. (1989) Primary structure of a putative receptor for a ligand of the insulin family. J. Biol. Chem. **264**, 14605–14608
29 Leconte, I., Auzan, C., Debant, A., Rossi, B. and Clauser, E. (1992) N-linked oligosaccharide chains of the insulin receptor beta subunit are essential for transmembrane signaling. J. Biol. Chem. **267**, 17415–17223
30 Collier, E., Carpentier, J.-L., Beitz, L., Caro, L. H. P., Taylor, S. I. and Gordon, P. (1993) Specific glycosylation site mutations of the insulin receptor α-subunit impair intracellular transport. Biochemistry **32**, 7818–7823
31 Caro, L. H. P., Ohali, A., Gorden, P and Collier, E. (1994) Mutational analysis of the NH_2-terminal glycosylation sites of the insulin receptor α-subunit. Diabetes **43**, 240–246
32 Bastian, W., Zhu, J., Way, B., Lockwood, D. and Livingston, J. (1993) Glycosylation of Asn397 or Asn418 is required for normal insulin receptor biosynthesis and processing. Diabetes **42**, 966–974
33 Stanley, P. (1989) Chinese hamster ovary cell mutants with multiple glycosylation defects for production of glycoproteins with minimal carbohydrate heterogeneity. Mol. Cell. Biol **9**, 377–383
34 Ellis, L., Clauser, E., Morgan, D. O., Edery, M., Roth, R. A. and Rutter, W. J. (1986) Replacement of insulin receptor tyrosine residues 1162 and 1163 compromises insulin-stimulated kinase activity and uptake of 2-deoxyglucose. Cell **45**, 721–732
35 Norrander, J., Kempe, T. and Messing, J. (1983) Construction of improved M13 vectors using oligodeoxynucleotide-directed mutagenesis. Gene **26**, 101–106
36 Carter, P. (1987) Improved oligonucleotide-directed mutagenesis using M13 vectors. Methods Enzymol. **154**, 382–403

37 Sanger, F., Nicklen, S. and Coulson, A. R. (1977) DNA sequencing with chain-terminating inhibitors. Proc. Natl. Acad. Sci. U.S.A. **74**, 5463–5467
38 Bebbington, C. R. and Hentschel, C. C. G. (1987) The use of vectors based on gene amplification for the expression of cloned genes in mammalian cells. In DNA Cloning, vol. 3 (Glover, D., ed.), pp. 163–188, IRL Press, Oxford
39 Soos, M. A., Siddle, K. and Baron, M. D. (1986) Monoclonal antibodies reacting with multiple epitopes on the human insulin receptor. Biochem. J. **235**, 199–208
40 Lammers, R., Gray, A., Schlessinger, J. and Ullrich, A. (1989) Differential signalling potential of insulin- and IGF-1-receptor cytoplasmic domains. EMBO J. **8**, 1369–1375
41 Laemmli, U. K. (1970) Cleavage of structural proteins during the assembly of the head of bacteriophage T4. Nature (London) **227**, 680–685
42 Whittaker, J., Garcia, P., Yu, G. Q. and Mynarcik, D. C. (1994) Transmembrane domain interactions are necessary for negative cooperativity of the insulin receptor. Mol. Endocrinol. **8**, 1521–1527
43 Munson, P. J. and Rodbard, D. (1980) Ligand: a versatile computerized approach for characterization of ligand-binding systems. Anal. Biochem. **107**, 220–239
44 Scatchard, G. (1949) The attractions of proteins for small molecules and ions. Ann. N. Y. Acad. Sci. **51**, 660–672
45 Bass, J. and Steiner, D. F. (2000) Insulin receptor folding. In Insulin Signalling: From Cultured Cells to Animal Models (Grunberger, G. and Zick, Y., eds.), Harwood Academic Press, New York, in the press
46 Olson, T. S., Bamberger, M. J. and Lane, M. D. (1988) Post-translational changes in tertiary and quaternary structure of the insulin proreceptor. Correlation with acquisition of function. J. Biol. Chem. **263**, 7342–7351
47 Helenius, A. (1994) How N-linked oligosaccharides affect glycoprotein folding in the endoplasmic reticulum. Mol. Biol. Cells **5**, 253–265
48 Wiese, R. J., Herrera, R. and Lockwood, D. H. (1995) Glycosylation sites encoded by exon 2 of the human insulin receptor gene are not required for the oligomerization, ligand binding, or kinase activity of the insulin receptor. Receptor **5**, 71–80
49 Schumacher, R., Soos, M. A., Schlessinger, J., Brandenburg, D., Siddle, K. and Ullrich, A. (1993) Signaling-competent receptor chimeras allow mapping of major insulin receptor binding domain determinants. J. Biol. Chem. **268**, 1087–1094
50 Fabry, M., Schaefer, E., Ellis, L., Kojro, E., Fahrenholz, F. and Brandenburg, D. (1992) Detection of a new hormone contact site within the insulin receptor ectodomain by the use of a novel photoreactive insulin. J. Biol. Chem. **267**, 8950–8956

Received 6 December 1999/7 February 2000; accepted 29 February 2000